Liposome Supported Metal Oxide Nanoparticles: Interaction Mechanism, Light Controlled Content Release and Intracellular Delivery

Feng Wang and Juewen Liu*

Department of Chemistry, Waterloo Institute for Nanotechnology, University of Waterloo, Waterloo, Ontario, Canada, N2L 3G1

Email: liujw@uwaterloo.ca

This is the peer reviewed version of the following article: Wang, F. and Liu, J. (2014), Liposome Supported Metal Oxide Nanoparticles: Interaction Mechanism, Light Controlled Content Release, and Intracellular Delivery. Small, 10: 3927–3931. doi:10.1002/smll.201400850, which has been published in final form at http://dx.doi.org/10.1002/smll.201400850. This article may be used for non-commercial purposes in accordance with Wiley Terms and Conditions for Self-Archiving.

Lipid-functionalized hybrid nanomaterials are highly attractive. Receptors, ion channels and targeting ligands can be incorporated into fluid bilayers to promote cell differentiation, sensing and targeted drug delivery.[1-7] In turn, introducing inorganic components to liposomes opens new possibilities for drug delivery, allowing enhanced drug loading, optical or magnetic diagnosis, improved bilayer stability, and controlled content release.[8-12] Since the surface chemistry of each inorganic material is different, they interact with lipids via a variety of mechanisms. On silica and mica, lipids form supported bilayers, where van der Waals force is important.[13-15] On graphene, liposomes either stably adsorb or undergo fusion, depending on the level of graphene oxidation and liposome surface charge,[16-20] in which hydrogen bonding and hydrophobic interactions are critical. Gold nanoparticles (NPs) with various surface modifications interact with liposomes by electrostatic adsorption or hydrophobic forces.[21] In addition, cationic particles often induce defects and damage lipid membranes, displaying strong cytotoxicity.[22]

Metal oxide nanoparticles have attracted considerable interest in medical fields. For example, titanium is one of the most promising implant materials due to its mechanical properties and excellent biocompatibility attributable to its native surface oxide layer.[23] The photocatalytic property of TiO_2 NPs have been exploited for antibacterial and cancer treatment.[24,25] Iron oxide is approved for treating iron deficiency, which supports its safety. It is also used for cell separation, immunoassays, magnetic resonance imaging, and hyperthermia therapy.[26,27] ZnO is also an attractive material for making biosensors and is a main ingredient of sunscreens due to its UV absorbing property.[28]

To date, a few reports studied hybrid materials made of metal oxides and lipids.[29-39] However, most previous work employed bulk planar surfaces, while little is known about interactions with oxide NPs. Among the different methods to construct hybrid materials (e.g. covalent conjugation, entrapment and adsorption), we are interested in adsorption due to its simplicity and cost-effectiveness. Herein, we report hybrid materials formed by liposomes and three medically important oxides (TiO_2, ZnO and

Fe_3O_4, see Figure 1A). SiO_2 NPs were also included for comparison. Their fundamental interaction mechanisms and applications have been explored.

The oxides used in this study are nanocrystalline as indicated by X-ray diffraction (XRD, Figure S1), except for SiO_2, which is amorphous. Their sizes are in the range between 20 and 50 nm determined by TEM (Figure S2). Zwitterionic DOPC liposomes (see Figure 1B for structure) are employed because of its excellent biocompatibility. Our DOPC liposomes have an average size of ~100 nm based on dynamic light scattering (DLS, Figure S3). To test whether the oxides can be associated with liposomes by simple adsorption, rhodamine-labeled DOPC liposomes were mixed with each oxide. After centrifugation, we observed the loss of fluorescence in the supernatant (Figure 1C). This indicates liposome adsorbed by all the oxides and oxide/liposome hybrids were formed. Control experiments showed that free DOPC liposomes cannot be precipitated at this centrifugation speed (Figure S4). From the fundamental materials science standpoint, we need to first understand the interacting force between this zwitterionic lipid and the oxides.

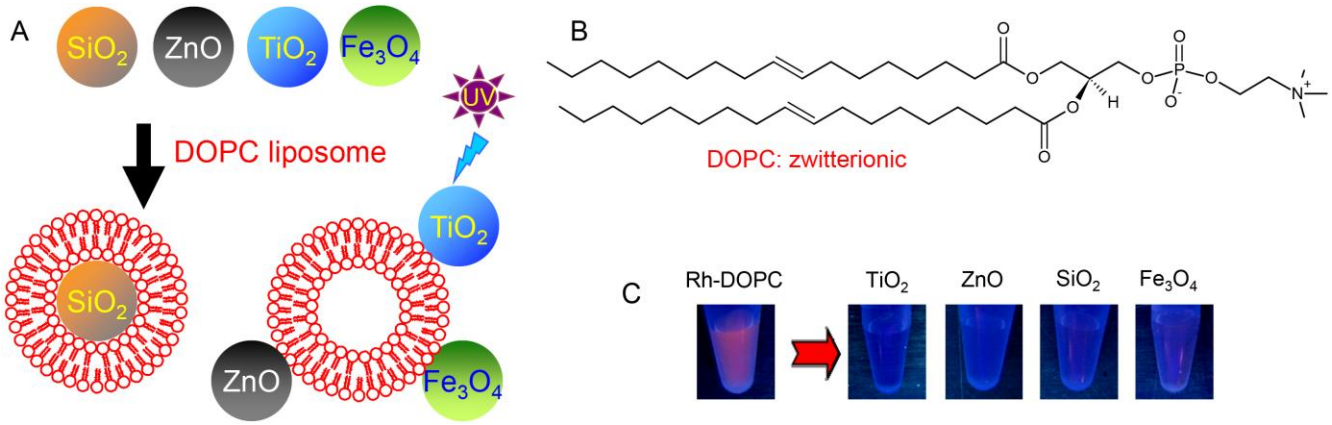

Figure 1. (A) Hybrid materials formed using the oxides and DOPC liposomes. SiO_2 NPs form supported bilayers, while the other oxides are adsorbed. TiO_2 is a photocatalyst. (B) Structure of the DOPC lipid. (C) Rh-DOPC liposome adsorption by the oxides indicated by the change of supernatant

fluorescence intensity. For the Fe_3O_4 NPs, the separation of supernatant was achieved by a magnet instead of centrifugation.

The interaction between DOPC and silica NPs is well established, where the liposome fuses onto the particle forming supported bilayers. However, interactions with other metal oxides are less developed. We first tested the effect of salt concentration (Figure 2A). For TiO_2, the amount of adsorbed DOPC is quite insensitive to ionic strength (black bars); each 100 μg of TiO_2 NPs attracts ~20 μg DOPC. For comparison, DOPC adsorption by SiO_2 NPs is promoted by NaCl (gray bars). This suggests a mechanistic difference in DOPC interacting with TiO_2 and SiO_2. This study also argues against electrostatic attraction for TiO_2 adsorption. Otherwise, a higher salt concentration should give a lower capacity due to charge screening. This also agrees with the zwitterionic nature of DOPC (overall charge neutral). Non-electrostatic interactions are interesting, since they avoid toxic cationic components.

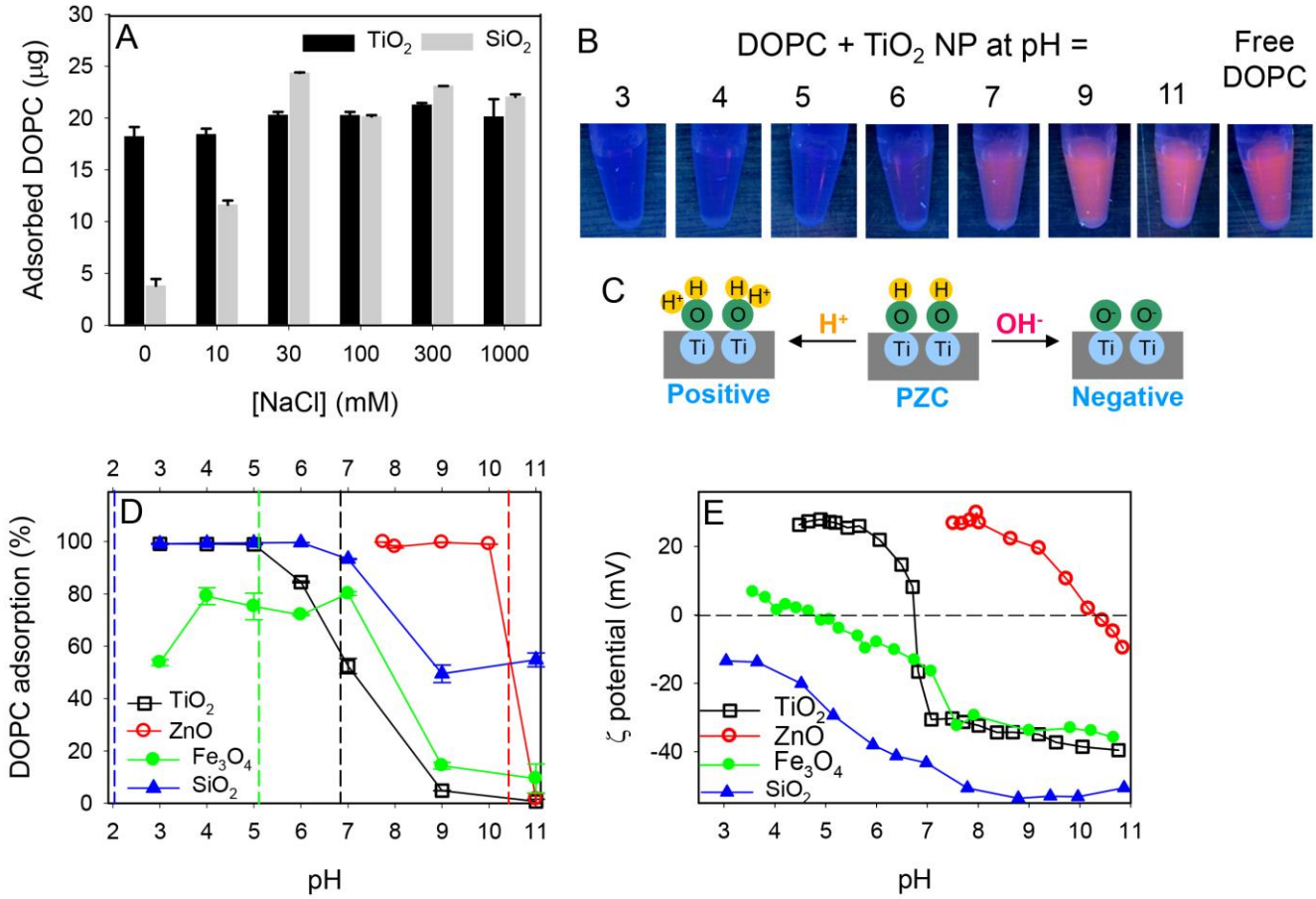

Figure 2. (A) The mass of DOPC associated with 100 μg of TiO_2 or SiO_2 NPs as a function of NaCl concentration. (B) Photographs of Rh-labeled DOPC liposome interacting with TiO_2 NPs as a function of pH. High fluorescence indicates weak interaction. (C) A scheme of protonation of TiO_2, affecting its surface charge. (D) Quantification of DOPC adsorption by various oxides as a function of pH. The dashed vertical lines represent the PZC of the oxides. The error bars represent standard deviation from three independent measurements. (E) ζ-potential as a function of pH for the oxides. The SiO_2 sample contained 10 mM NaCl.

To further understand the interaction mechanism, we studied the effect of pH. For TiO_2 NPs, the interaction was significantly weakened at pH higher than 7 (Figure 2B). This pH-dependent trend is true for all the oxides (Figure 2D), but the onset of inhibition is different in each case. To understand

the effect of surface charge, we measured the ζ-potential of the oxides as a function of pH. The oxide surfaces are capped by -OH groups at their point of zero charge (PZC); they become positively charged at lower pH and negatively charged at higher pH (Figure 2C). TiO_2 has a PZC at pH 6.8 (Figure 3D), while this transition takes place at pH 10 for ZnO. These PZC are indicated by the dashed vertical lines in Figure 2D. A reasonable agreement is found between the onset of losing DOPC and the surface becoming negatively charged. The only exception is SiO_2, which is negatively charged at pH higher than 2.[40] It retains partial DOPC adsorption even at pH 11. From pH 3 and above, the lipid head group maintains an overall neutral charge, and the effect of pH must be acting on the oxide surface. Taken together, when the metal oxides (excluding SiO_2) are negatively charged at high pH, DOPC binding is inhibited. On the low pH side after passing their PZC, all the oxides adsorb DOPC effectively. Although high pH inhibits oxide-DOPC interaction, once formed at low pH, the hybrid materials remain stable at high pH (Figure S5). Therefore, high pH only poses a kinetic barrier.

Since electrostatic interaction is unlikely to play a major role, we next probed chemical interactions. Based on the structure of PC head group containing a choline and a phosphate, we added free phosphate or choline salts to the oxides before mixing them with DOPC (Figure 3A). Interestingly, phosphate inhibited DOPC adsorption to all the oxides, except for SiO_2. On the other hand, choline had no effect. Therefore, it is likely that the phosphate part of the lipid head group interacts directly with the metal oxides.

Based on the above observations, we propose a mechanism of DOPC adsorption by the metal oxides (Figure 3C). Using TiO_2 as an example, the lipid phosphate oxygen performs a nucleophilic attack at the Ti center forming a covalent linkage. Bonding between the phosphate and the TiO_2 surface is also supported by IR spectroscopy (Figure S6). This mechanism can explain the pH trend. When the surface is negatively charged at high pH, it is more difficult for the negatively charged lipid phosphate to perform the attack. Therefore, acidic pH is optimal for adsorption. Since it is strong chemical bonding, once formed at low pH, it remains stable at high pH. Since phosphate inhibits DOPC

adsorption by TiO_2, ZnO and Fe_3O_4, they are likely to share the same reaction mechanism. It needs to be noted that adsorption to SiO_2 is different, where free phosphate fails to inhibit. It is known that a ~1 nm water layer separates PC lipids and silica. In other words, these two surfaces do not contact directly and they interact via van der Waals force (Figure 3D).[13] The fundamental reason for this difference might be related to the highly negatively charged surface of SiO_2, wherein physisorption becomes energetically more favorable.

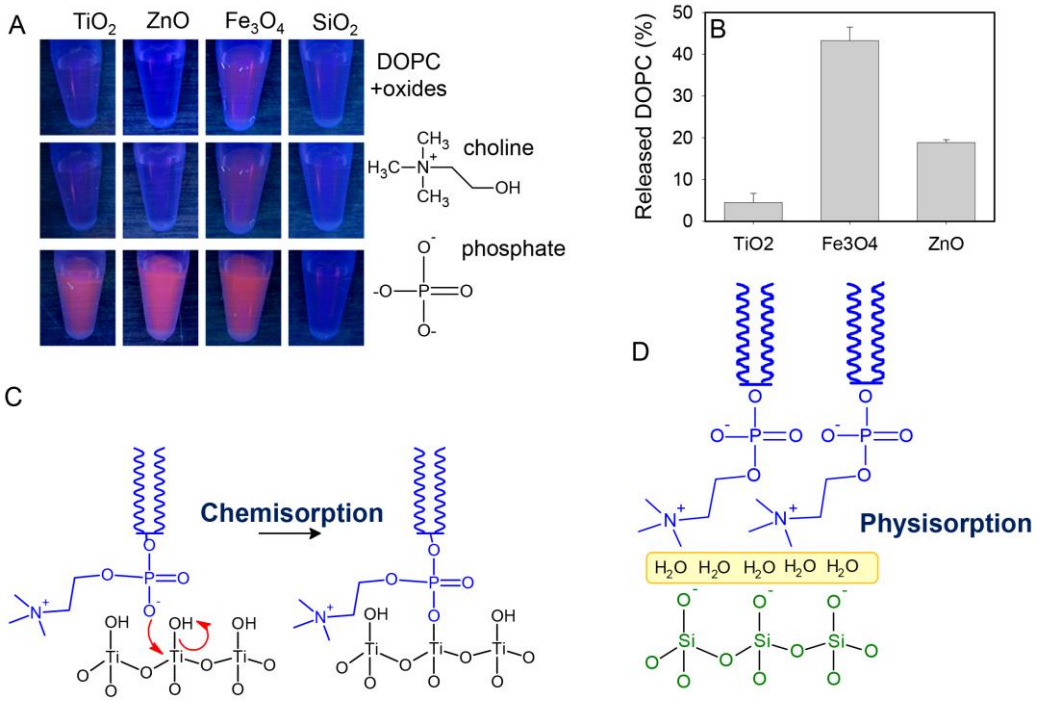

Figure 3. Photographs showing that DOPC adsorption by the metal oxides (excluding SiO_2) is inhibited by phosphate but not choline. Phosphate does not inhibit SiO_2 adsorption. (B) Displacement of adsorbed DOPC liposomes from the oxides by 20 mM free phosphate, showing Fe_3O_4 adsorption is the weakest. The error bars represent standard deviation from three independent measurements. (C) Proposed reaction mechanism for chemisorption of DOPC by TiO_2. (D) Schematics of PC liposome physisorption on silica separated by a thin water layer.

To test the stability of the hybrid materials, we next challenged the DOPC/oxide conjugates with free phosphate ions, and the amount of released DOPC was quantified (Figure 3B). TiO_2 adsorbs

DOPC the most tightly since only 5% liposome was released, while Fe_3O_4 adsorption was the weakest. Nevertheless, more than 50% of DOPC was still retained in the presence of 20 mM phosphate. Such stable hybrid materials formed by a simple mixing step are useful for drug delivery.

After understanding the mechanism of association, we next studied liposome integrity using cryo-TEM. Indeed, all the silica NPs are wrapped with a lipid bilayer (Figure 4A), consistent with its known lipid fusion mechanism. We also observed the intermediate fusion steps, where Figure 4B shows the starting and Figure 4C shows the ending of such a process. On the other hand, spherical intact liposomes are associated with TiO_2 (Figure 4D), Fe_3O_4 (Figure 4E), and ZnO (Figure 4F) with no evidence of supported bilayer formation. This experiment also confirms a different interaction mechanism between silica and the rest of the oxides.

Zwitterionic PC lipids are known for their antifouling property,[41] but they can still adsorb a diverse range of nanomaterials including latex beads and graphene oxide.[42-44] However, the interaction mechanism is not always clear, impeding the further development of more advanced materials by rational design. In this study, we demonstrated a new mechanism for interacting with metal oxides, which are medically important materials.

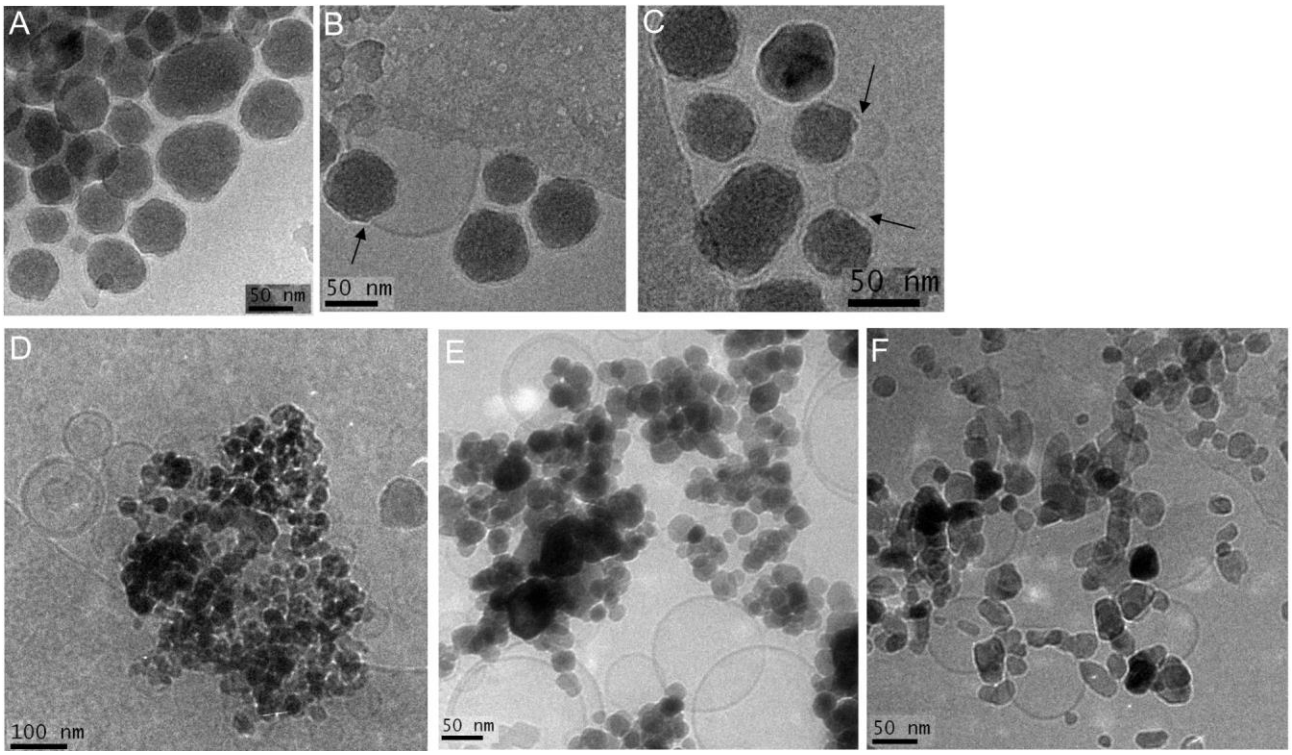

Figure 4. Cryo-TEM micrographs of DOPC mixed with SiO_2 NPs (A, B, C). The arrow heads in (B, C) point at the intermediate processes of liposome fusion with the particles. DOPC with TiO_2 (D), Fe_3O_4 (E) and ZnO (F).

Overall, at least two types of hybrid materials can form between oxides and DOPC liposomes (Figure 1A). With silica, the supported bilayer mimics a cellular compartment,[45] where it is appropriate to incorporate functional proteins within the bilayer. Since intact liposomes are associated with the other oxides, controlled release might be achieved.

Each oxide has its own physical property, which may enable unique applications when conjugated to liposomes. In this initial study, we focus on the photocatalytic property of TiO_2 NPs. We loaded a high concentration of calcein to DOPC liposomes, which are stable under UV light exposure (Figure 5A). At 30 min, Triton X-100 was added to fully rupture the liposome membrane, inducing a large fluorescence enhancement. Next, TiO_2 NPs and calcein loaded DOPC liposomes were mixed. After UV explosion, fluorescence increase was observed. Higher TiO_2 concentration induces more

leakage (Figure S7). On the other hand, Fe_3O_4 did not show increase fluorescence, since it lacks the photocatalytic activity. We next studied the effect of wavelength on the DOPC/TiO_2 conjugate and fluorescence increase was suppressed at longer wavelengths (Figure 5B). In particular, little release was generated under 600 nm light exposure. These experiments confirmed the photocatalytic role of TiO_2 in membrane leakage under UV exposure.

Finally, we tested cellular uptake. Free Rh-DOPC liposomes were not internalized by HeLa cells and no red fluorescence was observed (Figure 5C). This is related to the excellent biocompatibility of PC lipids and its anti-fouling nature to resist protein adsorption. On the other hand, strong red spot fluorescence was observed with Rh-DOPC/TiO_2 (Figure 5D). Staining acidic vesicles in the cells suggests that the particles are internalized by endocytosis (Figure S8). Rh-DOPC/SiO_2 and Rh-DOPC/Fe_3O_4 can also be internalized (Figure S9). This study confirms that the conjugates are stable enough to survive the cell culture conditions. In addition, the oxides facilitate the cellular uptake of the DOPC liposomes. Next we used calcein as a model drug, which by itself cannot be internalized by cells.[45] We incubated the cells with calcein-loaded DOPC/TiO_2. After 4 h, strong green fluorescence was associated with the cells, confirming the delivery effect (Figure 5E). Among all these oxides, only ZnO showed toxicity (Figure S10), while the others are highly biocompatible.

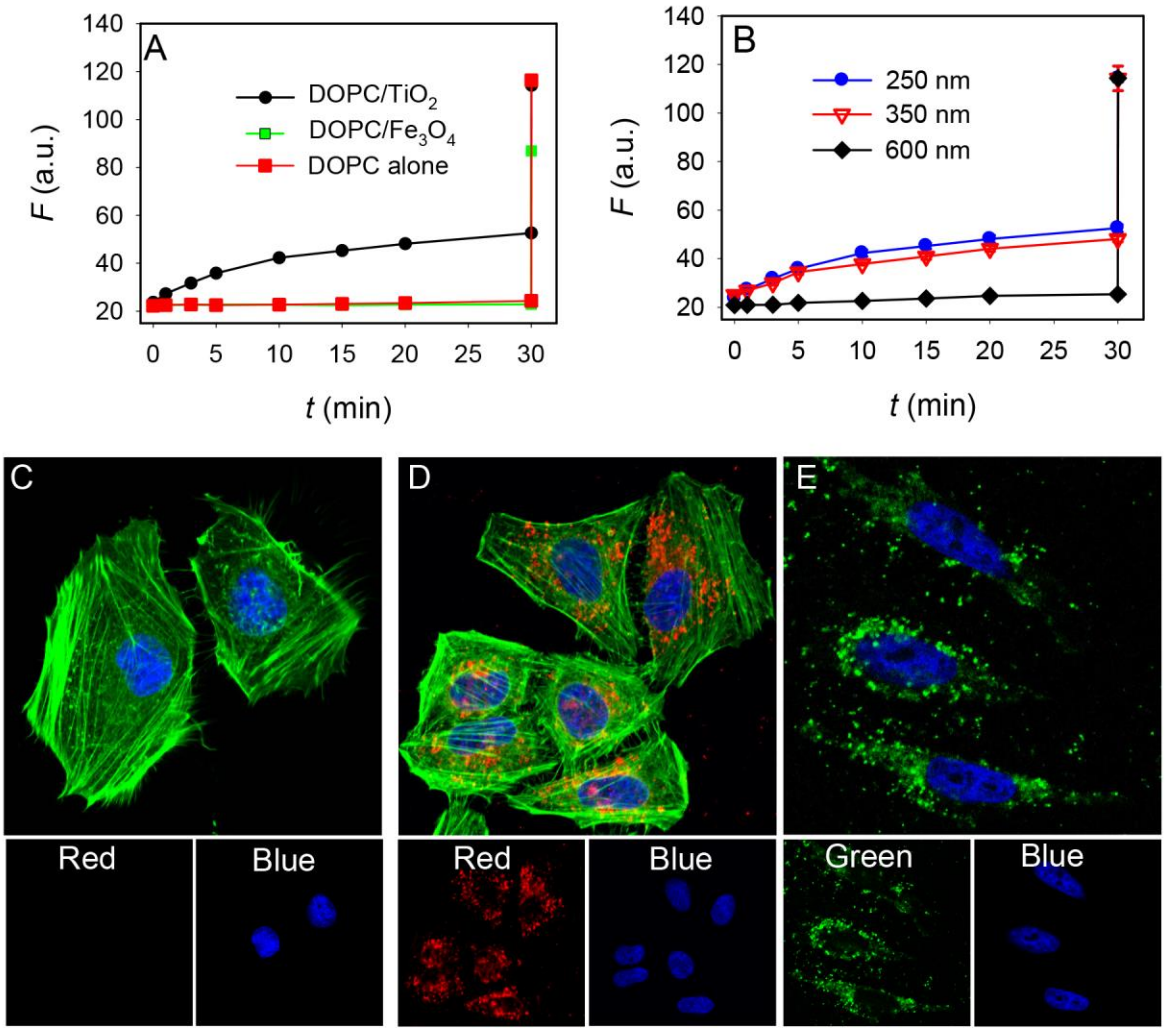

Figure 5. (A) UV-induced leakage of calcein loaded DOPC liposomes in the presence of TiO_2 and Fe_3O_4 NPs. (B) Effect of wavelength on the leakage of calcein-loaded DOPC in the presence of TiO_2. Confocal fluorescence micrographs of HeLa cells incubated with free Rh-DOPC liposomes (C), Rh-DOPC/TiO_2 (D), and calcein-DOPC/TiO_2 (E) for 4 h. The cytoskeleton actin was stained in green in (C, D) and the nuclei were stained in blue. The two smaller panels in each group are from the individual channels.

In summary, we studied the interaction between three medically important oxides and a highly biocompatible liposome. A new mechanism was proposed to describe their interaction, in which the

phosphate in the lipid head group directly bonds with the metal oxide surface. TiO_2 interacting with phosphate in biomolecules was also reported for DNA.[46] This strong chemical interaction is very different from the van der Waals force for silica adsorption, where a thin water layer separates silica surface from the liposome surface. Without the water layer, direct bonding leads to a large steric hindrance, impeding liposome rupture and the formation of supported bilayers. For example, the choline group causes strong steric effects if DOPC fuses on TiO_2 surface since the lipid phosphate needs to bond to the surface directly. The DOPC/oxide conjugates are stable enough to be taken by cells and the photocatalytic activity of TiO_2 NPs is harnessed to achieve light controlled liposome content release. This study significantly expands the range of materials used to form lipid interfaces and will find applications in biosensor development, drug delivery, device fabrication, as well as enabling new fundamental biophysical studies. Finally, we revealed the importance of phosphate in lipid in interacting with surfaces, which may lead to new thoughts on materials design using liposomes as a template.

Supporting Information. Materials and methods, XRD, liposome leakage and cell viability assays, DLS. Supporting Information is available from the Wiley Online Library or from the author.

ACKNOWLEDGMENT

We thank Quanquan Pang for assistance with XRD measurement. Funding for this work is from the University of Waterloo, CFI, Early Researcher Award from Ontario Ministry of Research & Innovation, and the NSERC of Canada.

References:

[1] E. Sackmann, *Science* **1996**, *271*, 43.

[2] J. L. Vivero-Escoto, R. C. Huxford-Phillips, W. B. Lin, *Chem. Soc. Rev.* **2012**, *41*, 2673.

[3] M. J. Sailor, J.-H. Park, *Adv. Mater.* **2012**, *24*, 3779.

[4] S. Tan, X. Li, Y. Guo, Z. Zhang, *Nanoscale* **2012**, *5*, 860.

[5] W. Gao, C.-M. J. Hu, R. H. Fang, L. Zhang, *J. Mater. Chem. B* **2013**, *1*, 6569.

[6] L. Yang, X. B. Zhang, M. Ye, J. H. Jiang, R. H. Yang, T. Fu, Y. Chen, K. M. Wang, C. Liu, W. H. Tan, *Adv. Drug Deliver. Rev.* **2011**, *63*, 1361.

[7] H. Wang, R. H. Yang, L. Yang, W. H. Tan, *ACS Nano* **2009**, *3*, 2451.

[8] C. E. Ashley, E. C. Carnes, G. K. Phillips, D. Padilla, P. N. Durfee, P. A. Brown, T. N. Hanna, J. Liu, B. Phillips, M. B. Carter, N. J. Carroll, X. Jiang, D. R. Dunphy, C. L. Willman, D. N. Petsev, D. G. Evans, A. N. Parikh, B. Chackerian, W. Wharton, D. S. Peabody, C. J. Brinker, *Nat. Mater.* **2011**, *10*, 389.

[9] D. Pornpattananangkul, L. Zhang, S. Olson, S. Aryal, M. Obonyo, K. Vecchio, C.-M. Huang, L. Zhang, *J. Am. Chem. Soc.* **2011**, *133*, 4132.

[10] X. Liang, X. Li, X. Yue, Z. Dai, *Angew. Chem., Int. Ed.* **2011**, *50*, 11622.

[11] Z. Cao, X. Yue, X. Li, Z. Dai, *Langmuir* **2013**, *29*, 14976.

[12] V. Cauda, H. Engelke, A. Sauer, D. Arcizet, C. Brauchle, J. Radler, T. Bein, *Nano Lett.* **2010**, *10*, 2484.

[13] P. S. Cremer, S. G. Boxer, *J. Phys. Chem. B* **1999**, *103*, 2554.

[14] S. p. Mornet, O. Lambert, E. Duguet, A. Brisson, *Nano Lett.* **2004**, *5*, 281.

[15] A. M. Carmona-Ribeiro, *Chem. Soc. Rev.* **2001**, *30*, 241.

[16] A. V. Titov, P. Kral, R. Pearson, *ACS Nano* **2009**, *4*, 229.

[17] P. K. Ang, M. Jaiswal, C. H. Y. X. Lim, Y. Wang, J. Sankaran, A. Li, C. T. Lim, T. Wohland, O. Barbaros, K. P. Loh, *ACS Nano* **2010**, *4*, 7387.

[18] R. Frost, G. E. Jonsson, D. Chakarov, S. Svedhem, B. Kasemo, *Nano Lett.* **2012**, *12*, 3356.

[19] A. C. F. Ip, B. Liu, P.-J. J. Huang, J. Liu, *Small* **2013**, *9*, 1030.

[20] Y. S. Tu, M. Lv, P. Xiu, T. Huynh, M. Zhang, M. Castelli, Z. R. Liu, Q. Huang, C. H. Fan, H. P. Fang, R. H. Zhou, *Nat. Nanotechnol.* **2013**, *8*, 594.

[21] A. Verma, F. Stellacci, *Small* **2010**, *6*, 12.

[22] P. R. Leroueil, S. A. Berry, K. Duthie, G. Han, V. M. Rotello, D. Q. McNerny, J. R. Baker, B. G. Orr, M. B. Banaszak Holl, *Nano Lett.* **2008**, *8*, 420.

[23] L. L. Hench, *Curr. Opin. Solid St. M.* **1997**, *2*, 604.

[24] L. Ye, R. Pelton, M. A. Brook, C. D. M. Filipe, H. F. Wang, L. Brovko, M. Griffiths, *Bioconjug. Chem.* **2013**, *24*, 448.

[25] J.-w. Seo, H. Chung, M.-y. Kim, J. Lee, I.-h. Choi, J. Cheon, *Small* **2007**, *3*, 850.

[26] Q. A. Pankhurst, J. Connolly, S. K. Jones, J. Dobson, *J. Phys. D-Appl. Phys.* **2003**, *36*, R167.

[27] A. K. Gupta, M. Gupta, *Biomaterials* **2005**, *26*, 3995.

[28] G. J. Nohynek, J. Lademann, C. Ribaud, M. S. Roberts, *Crit. Rev. Toxicol.* **2007**, *37*, 251.

[29] I. Reviakine, F. F. Rossetti, A. N. Morozov, M. Textor, *J. Chem. Phys.* **2005**, *122*, 204711.

[30] R. Tero, T. Ujihara, T. Urisut, *Langmuir* **2008**, *24*, 11567.

[31] N. J. Cho, C. W. Frank, *Langmuir* **2010**, *26*, 15706.

[32] C. A. Keller, K. Glasmastar, V. P. Zhdanov, B. Kasemo, *Phys. Rev. Lett.* **2000**, *84*, 5443.

[33] F. F. Rossetti, M. Textor, I. Reviakine, *Langmuir* **2006**, *22*, 3467.

[34] F. F. Rossetti, M. Bally, R. Michel, M. Textor, I. Reviakine, *Langmuir* **2005**, *21*, 6443.

[35] T. Khan, H. M. Grandin, A. Mashaghi, M. Textor, E. Reimhult, I. Reviakine, *Biointerphases* **2008**, *3*, FA90.

[36] M. J. Scott, M. N. Jones, *Colloid. Surface. A.* **2002**, *207*, 69.

[37] N.-J. Cho, J. A. Jackman, M. Liu, C. W. Frank, *Langmuir* **2011**, *27*, 3739.

[38] E. Reimhult, F. Hook, B. Kasemo, *Langmuir* **2002**, *19*, 1681.

[39] B. Denizot, G. Tanguy, F. Hindre, E. Rump, J. Jacques Le Jeune, P. Jallet, *J. Colloid Interf. Sci.* **1999**, *209*, 66.

[40] C. J. Brinker, G. W. Scherer, *Sol-Gel Science: The Physics and Chemistry of Sol-Gel Processing*, Academic Press, Boston **1990**.

[41] S. F. Chen, S. Y. Jiang, *Adv. Mater.* **2008**, *20*, 335.

[42] A. L. Lewis, *Colloids and Surfaces B: Biointerfaces* **2000**, *18*, 261.

[43] B. Wang, L. F. Zhang, S. C. Bae, S. Granick, *Proc. Natl. Acad. Sci. U.S.A.* **2008**, *105*, 18171.

[44] L. F. Zhang, S. Granick, *Nano Lett.* **2006**, *6*, 694.

[45] J. Liu, A. Stace-Naughton, X. Jiang, C. J. Brinker, *J. Am. Chem. Soc.* **2009**, *131*, 1354.

[46] X. Zhang, F. Wang, B. Liu, E. Y. Kelly, M. R. Servos, J. Liu, *Langmuir* **2014**, *30*, 839.